Stem Cell Reports, Volume *1*

Supplemental Information

Induced Pluripotent Stem Cell Modeling of Multisystemic, Hereditary Transthyretin Amyloidosis

Amy Leung, Shirley K. Nah, Whitney Reid, Atsushi Ebata, Clarissa M. Koch, Stefano Monti, Joseph C. Genereux, R. Luke Wiseman, Benjamin Wolozin, Lawreen H. Connors, John L. Berk, David C. Seldin, Gustavo Mostoslavsky, Darrell N. Kotton, and George J. Murphy

Supplemental Materials

Inventory of Supplemental Data.

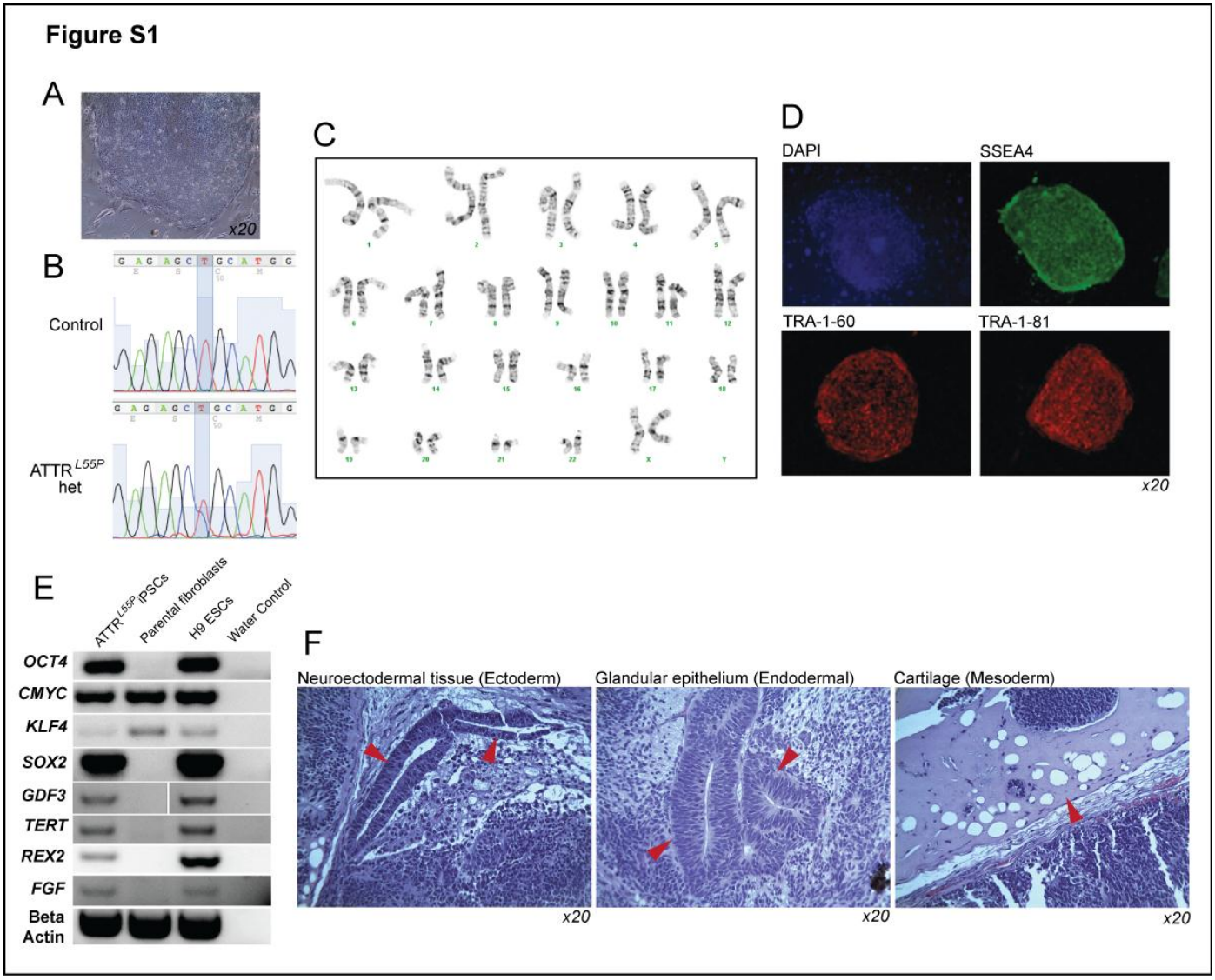

Figure S1. ATTR^{L55P} iPSC exhibit hallmarks of true pluripotent cells; related to Figure 1.

(A) ATTR^{L55P} iPSC exhibit typical iPSC colony morphology. (B) Sequencing of the TTR transcript generated from control iPSC/ATTR^{L55P} iPSC (hepatic) derivatives confirms that the ATTR^{L55P} cells are heterozygous for the L55P mutation (point mutation site highlighted in blue) (C) ATTR^{L55P} iPSC are karyotypically normal. (D) Immunofluoresence analysis shows that ATTR^{L55P} iPSC are positive for pluripotency markers SSEA4, TRA- 1-81 and TRA-1-60. (E) Semi-quantitative PCR analysis of gene expression in ATTR^{L55P} iPSC compared to the parental fibroblasts shows the upregulation of a host of pluripotency markers. H9 ESC cDNA was included as a positive control. (F) Teratoma formation assay. ATTR^{L55P} iPSC were combined with Matrigel and implanted subcutaneously into NOD-SCID mice and the resultant tumors harvested for histological analysis. H&E-stained tumor sections display structures representing all three germ layers (ectoderm: neuroectodermal tissue, endoderm: glandular epithelium, and mesoderm: cartilage; red arrowheads) indicating that the cells are functionally pluripotent.

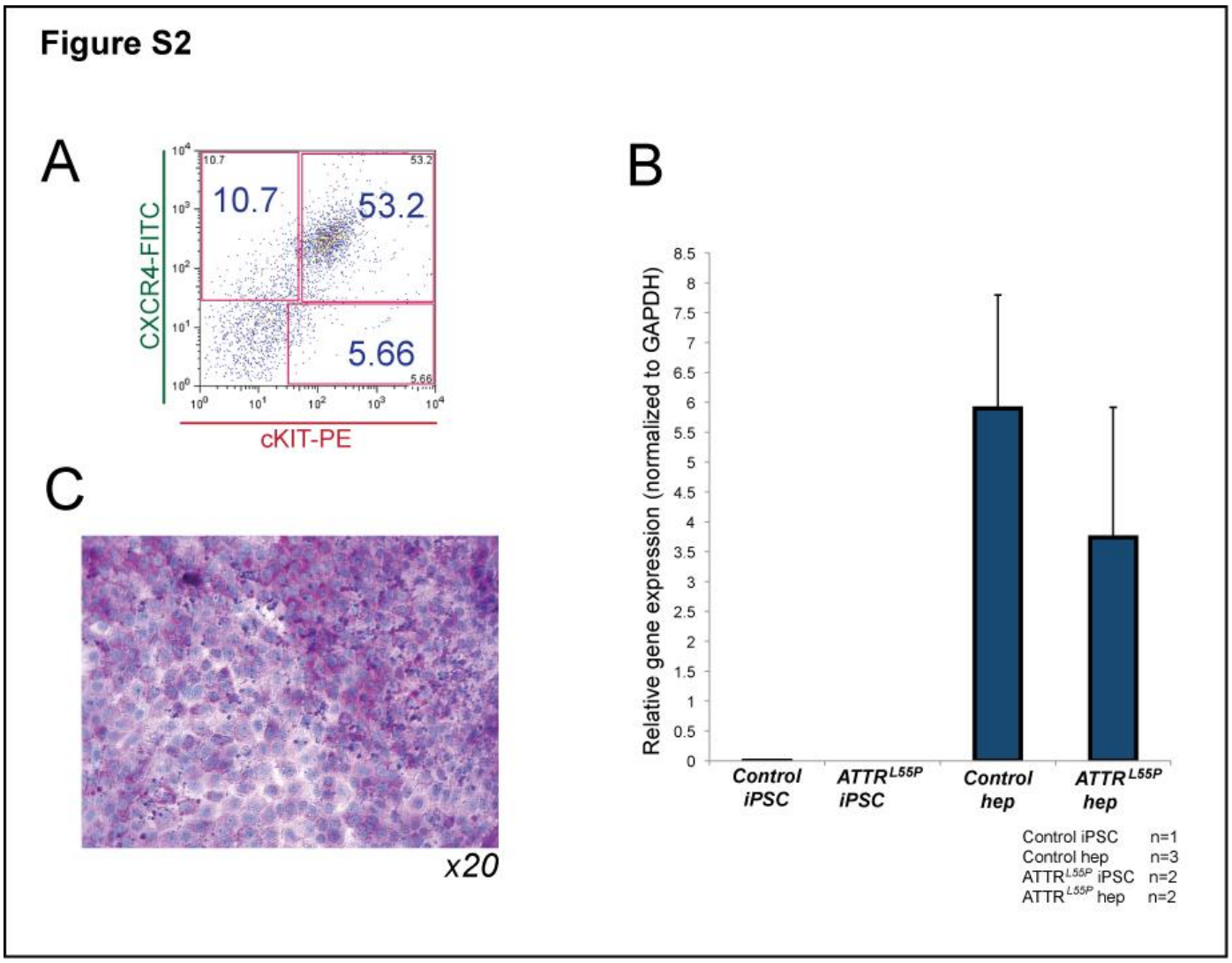

Figure S2. Characterization of control (WT) iPSC-derived hepatic lineage cells, related to Figure 2.

(A) After 5 days of differentiation, control iPSC (WT) express definitive endoderm cell surface markers, CXCR4 and cKit. (B) Quantitative PCR comparison of TTR gene expression in control versus ATTR^{L55P} iPSC and their hepatic-lineage derivatives. Readings were normalized to GAPDH. Sample sizes (independent biological replicates) are listed below the graph; error bars represent the standard deviation. (C) Control hepatic cells are capable of glycogen storage as assayed by PAS staining.

Figure S3

A

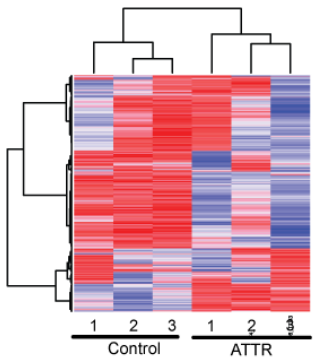

B

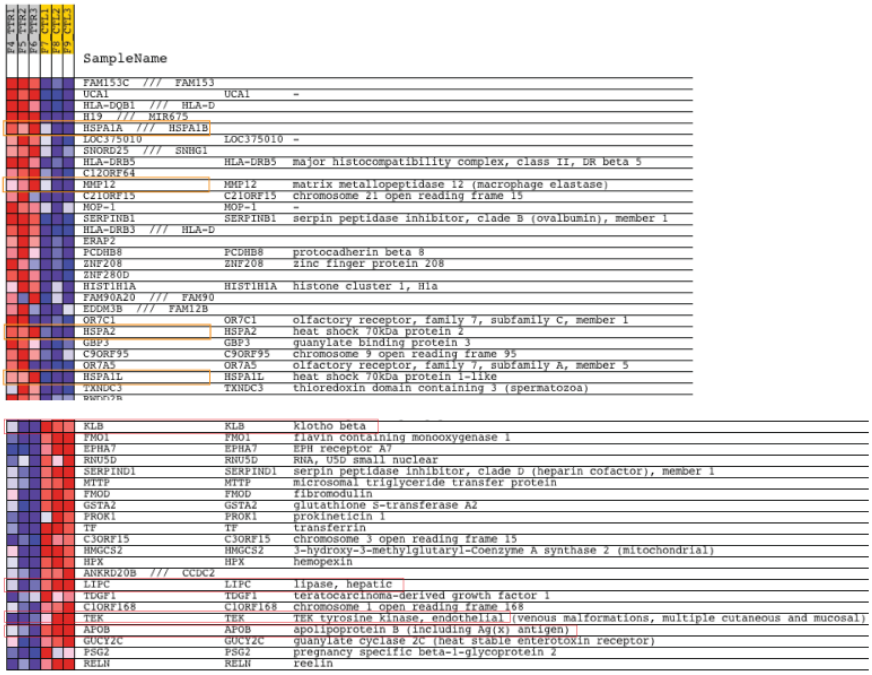

C

Connective tissue / coagulation genes		
Group with higher expression	Fold Change	
CTL	2.5	ADAMTS15 : ADAM metallopeptidase w/ TS type 1 motif, 15
CTL	1.85	FBN1 : fibrillin 1
CTL	1.99	COL4A1 : collagen, type IV, alpha 1
CTL	3.01	PLG : plasminogen
CTL	3.53	F2 : coagulation factor II (thrombin)
CTL	1.68	COL4A2 : collagen, type IV, alpha 2
Liver specific (metabolism)		
Group with higher expression	Fold Change	
TTR	1.48	CYP2E1 : cytochrome P450, family 2, subfamily E, polypeptide 1
CTL	2.84	APOC3 : apolipoprotein C-III
CTL	3.01	PLG : plasminogen
Protein folding		
Group with higher expression	Fold Change	
TTR	1.4	HSF2BP : heat shock transcription factor 2 binding protein
TTR	4.66	HSPA2 : heat shock 70kDa protein 2
CTL	5.64	KLB : klotho beta

D

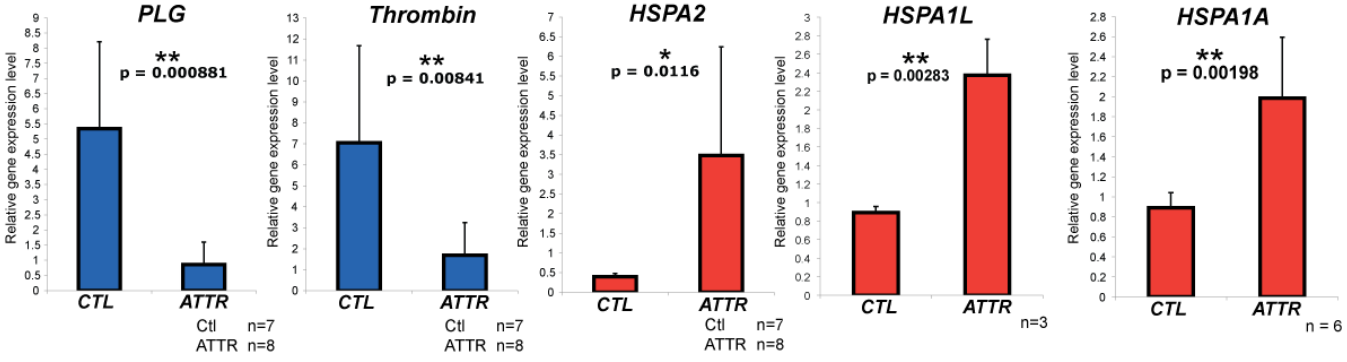

Figure S3. Comparative gene expression analysis of control and ATTR^{L55P} iPSC-derived hepatic cells, related to Figure 2.

(A) Hierachical clustering analysis of microarray data from control and $ATTR^{L55P}$ hepatic cells (3 biological replicates per set). The hepatic samples cluster according to their derivative cell type. (B) A select set of top dysregulated genes which differ between control and $ATTR^{L55P}$ hepatic lineage cell samples. Genes of interest relating to protein folding, stress response, connective tissue, and hepatic function are highlighted. (C) Grouping of differentially expressed genes based on function. (D) Quantitative PCR validation of particular genes of interest. Independent biological replicates were tested (n-values for each marker listed below each graph), and values were normalized to GAPDH. Error bars denote standard deviation. The significance level as determined by Student's t-test analysis is denoted in each graph.

Figure S4

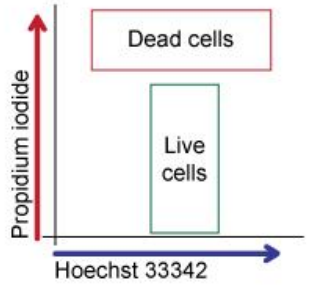
Dead cells
Live cells
Propidium iodide
Hoechst 33342

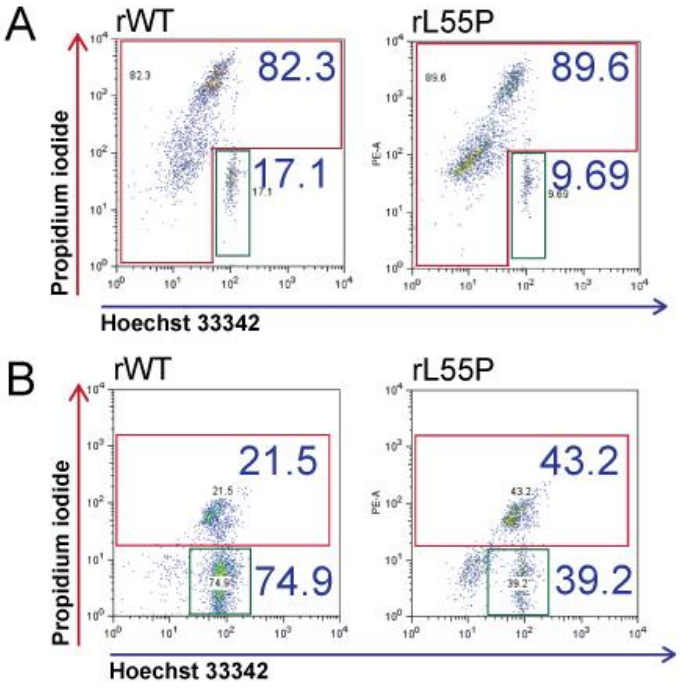
A
rWT
rL55P
82.3
17.1
89.6
9.69
Propidium iodide
Hoechst 33342
B
rWT
rL55P
21.5
74.9
43.2
39.2
Propidium iodide
Hoechst 33342

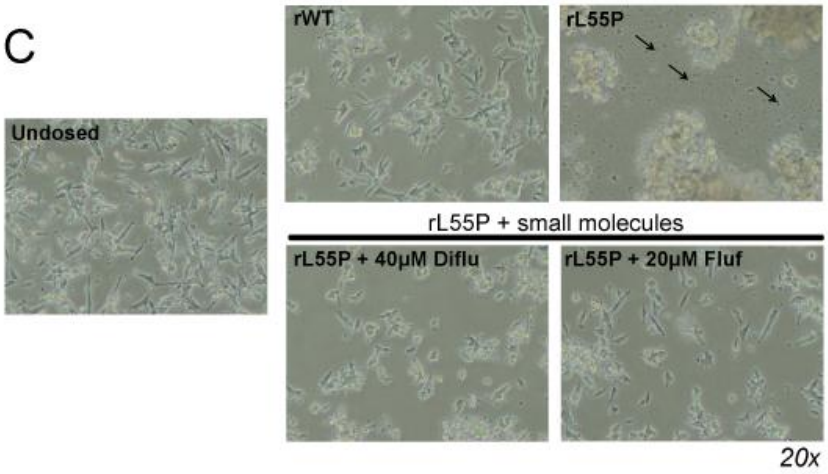
C
Undosed
rWT
rL55P
rL55P + small molecules
rL55P + 40μM Diflu
rL55P + 20μM Fluf
20x

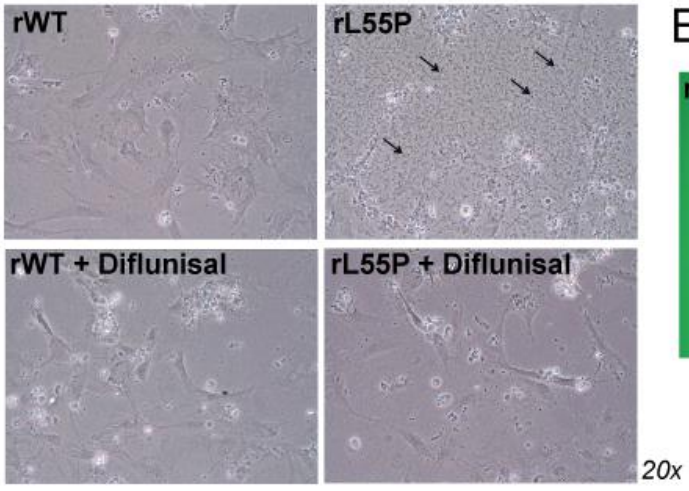
D
rWT
rL55P
rWT + Diflunisal
rL55P + Diflunisal
20x

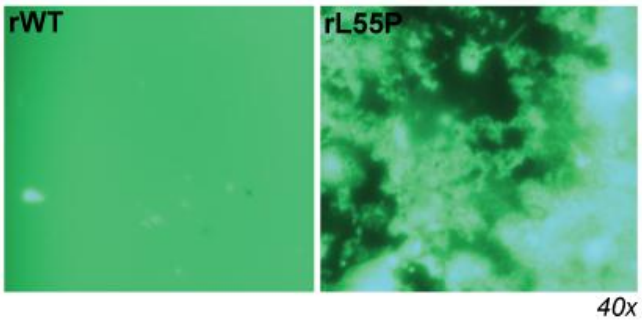
E
rWT
rL55P
40x

Figure S4. Modeling ATTR with the use of recombinant human TTR protein, related to Figure 5 and Figure 6.

(A) $ATTR^{L55P}$ neuronal cells exposed to rWT and rL55P proteins for 20 days were analyzed for PI and Hoechst 33342 uptake by flow cytometry. The percentage of live cells (the Hoechst positive gate, annotated) is decreased for cells exposed to rL55P protein. (B) $ATTR^{L55P}$ cardiac cells exposed to rWT and rL55P proteins for 21 days were analyzed for PI and Hoechst 33342 uptake by flow cytometry. The percentage of live cells (the Hoechst positive gate, annotated) is decreased for cells exposed to rL55P protein. (C) Neuroblastoma cells (SY5Y) were dosed with recombinant WT and L55P proteins, -/+ 40 μM diflunisal and 20 μM flufenamic acid, for 7 days. The rL55P cultures contained many small protein aggregates (examples highlighted with black arrows) and detached cell clumps, whereas cultures containing rL55P with the small molecules had no visible protein aggregates and fewer detached cells. (D) Phase contrast images of $ATTR^{L55P}$ iPSC-derived neuronal cell cultures after exposure to 0.2 mg/mL recombinant human TTR protein (rWT/rL55P) for 7 days. Many small aggregates (examples highlighted with black arrows) are visible in the culture containing rL55P protein; these are not seen in cultures containing WT protein. The addition of diflunisal (40 μM) to rL55P cultures prevented aggregate formation. (E) Thioflavin T staining of rWT and rL55P protein-dosed neuronal cultures revealed that the rL55P aggregates were amyloid protofilaments/fibrils that fluoresced when visualized with blue polarized light.

Transcript	FORWARD	REVERSE
GAPDH	GGAAATCCCATCACCATCTTCCAGG	GCAAATGAGCCCCAGCCTTCTC
NANOG	AGCCTCTACTCTTCCTACCACC	TCCAAAGCAGCCTCCAAGTC
OCT4	GACAACAATGAAAATCTTCAGGAGA	TTCTGGCGCCGGTTACAGAACCA
SOX17	GGACATGAAGGTGAAGGGCGAG	CTTGCCCAGCATCTTGCTCAACTC
FOXA2	CCAGTGGATCATGGACCTCTTCCC	CAGCTGCTTCTCGCACTTGAAGC
CKIT	CAGGCAACGTTGACTATCAGTTC	CTCAGACTTGGGATAATCTTCCC
CXCR4	GGAACCCTGTTTCCGTGAAGA	CTTGTCCGTCATGCTTCTCAG
AFP	CACCAGAAAAATGGCAGCCACA	CTGAGCTTGGCACAGATCCT
APOA1	ATCGAGTGAAGGACCTGGCC	AGCTTGCTGAAGGTGGAGGT
ALB	GCTGTGCCGCTGCAGATCCTCA	TGGAGTTGACACTTGGGGTAC
TTR	GCCGTGCATGTGTTCAGAAAG	GACAGCCGTGGTGGAATAGGA
Islet1	GTGGAGAGGGCCAGTCTAGG	CCGTCATCTCTACCAGTTGCT
Calponin	AAGGACGCACTGAGCAACGCTATT	ACGCCACTGTCACATCCACATAGT
cTNT	TTCACCAAAGATCTGCTCCTCGCT	TTATTACTGGTGTGGAGTGGGTGTGG
Cardiac muscle Actin	TCCCATCGAGCATGGTATCAT	GGTACGGCCAGAAGCATACA
TBX5	CATTGGATGAGGCAGCTCGTCTC	CGCAGTCTCAGGAAAGACGTGAGT
NKX2.5	GCCAAGGACCCTAGAGCCG	CAGGTACCGCTGCTGCTTGAAG
PDGFRa	TACCTGCCTCCTACGACAGCAG	CCTTTGCCTTTCACTTCTCCAGGG
P21	CTCAGGGTCGAAAACGGCG	AAGATGTAGAGCGGGCCTTTG
HO1	GCAGAGGGTGATAGAAGAGGC	CTTTGTTGCTGGCCCGCTG
MMP9	AGACGGGTATCCCTTCGACG	AAACCGAGTTGGAACCACGAC
RAGE	ACTACCGAGTCCGTGTCTACCAG	CCAAGTGCCAGCTAAGAGTCCC
HSPA1A	CTACTGCCAAGGGAATCGCC	GCCGATCAGACGTTTAGCATCA
HSPA1L	GGAGACAAGCCCAAGGTGCAG	GCGAGTCGTTGAAGTAGGCCG
Thrombin	CAGCTATGGAGGAGTCGCTAC	GCGTGGAGTCATCGCTACA
Klotho beta	ATGTCAGCAGCACGAATGGTT	GCGTTGGCAACTGTTACTATTCC
HSPA2	GGTCCCGGCCTATTTCAACG	GGACACGTCGAAAGTGCCA
PLG	TGTATCTCTCAGAGTGCAAGACT	CTGCGGATCGTTGTCTGGA
INOS	TTCAGTATCACAACCTCAGCAAG	TGGACCTGCAAGTTAAAATCCC
HSP27	TGGACCCCACCCAAGTTTC	CGGCAGTCTCATCGGATTTT
TNFALPHA	CCTCTCTCTAATCAGCCCTCTG	GAGGACCTGGGAGTAGATGAG
MCSF	AGACCTCGTGCCAAATTACATT	AGGTGTCTCATAGAAAGTTCGGA

Table S1. List of SYBRGreen quantitative PCR primers.

Experimental Procedures.

Microarray analysis of hepatic-lineage cells

Total RNA was extracted, then measured and quality-controlled on a Bioanalyzer. A total of 6 samples (3 control and 3 $ATTR^{L55P}$ hepatic-lineage cell samples; independent biological replicates) were profiled on Affymetrix human ST1.0 gene chips by the Boston University microarray core.. Probe-level data from the Affymetrix '.CEL' files were summarized using the Robust Multi-array Average (RMA) (Irizarry et al., 2003) procedure available through Bioconductor

(Gentleman et al., 2004), using a University of Michigan's custom CDF file based on Entrez annotation (hugene10stv1hsentrezgcdf, version 15) (Dai et al., 2005). Variation filtering was performed to reduce the initial number of 21,307 genes represented in the chip to the top 5000 genes as ranked by median absolute deviation (MAD) across conditions. Differential analysis with respect to the phenotype 'CTL vs. ATTR' was performed on the filtered dataset by performing a two-group t-test for each gene and by correcting the attained nominal p-values by the false discovery rate (FDR) procedure (Benjamini and Hochberg, 1995; Gould et al., 2006). Fold-change was also computed for each gene by taking the ratio of the within-group means. Hierarchical clustering on the dataset reduced to the top 1000 genes by MAD was performed using the Ward agglomeration rule, using the Euclidean distance for the sample clustering, and 1-Pearson correlation for the gene clustering (Eisen et al., 1998).

Recombinant TTR protein preparation

Recombinant human WT and L55P transthyretin proteins were prepared as previously described (Kingsbury et al., 2007). For dosing experiments involving recombinant TTR protein, the final concentration in media was 0.2mg/ml. Small molecule TTR stabilizers (diflunisal, flufenamic acid) were added to protein stocks and allowed to incubate at 4ºC overnight before dilution in media, filtration and addition to cell cultures. Labelling of WT and L55P recombinant TTR protein was carried out using an Alexa Fluor 488 Protein Labelling kit (Invitrogen) according to manufacturer recommendations. Neuronal and cardiac cells were dosed with media containing 0.2 mg/ml of labeled protein for 3 hours, washed and then visualized by fluorescence microscopy.

References.

Benjamini, Y., Hochberg, Y., 1995. Controlling the False Discovery Rate: A Practical and Powerful Approach to Multiple Testing. J. R. Stat. Soc. Ser. B Methodol. 57, 289–300.

Dai, M., Wang, P., Boyd, A.D., Kostov, G., Athey, B., Jones, E.G., Bunney, W.E., Myers, R.M., Speed, T.P., Akil, H., Watson, S.J., Meng, F., 2005. Evolving gene/transcript definitions significantly alter the interpretation of GeneChip data. Nucleic Acids Res. 33, e175.

Eisen, M.B., Spellman, P.T., Brown, P.O., Botstein, D., 1998. Cluster Analysis and Display of Genome-Wide Expression Patterns. Proc. Natl. Acad. Sci. 95, 14863–14868.

Gentleman, R.C., Carey, V.J., Bates, D.M., Bolstad, B., Dettling, M., Dudoit, S., Ellis, B., Gautier, L., Ge, Y., Gentry, J., Hornik, K., Hothorn, T., Huber, W., Iacus, S., Irizarry, R., Leisch, F., Li, C., Maechler, M., Rossini, A.J., Sawitzki, G., Smith, C., Smyth, G., Tierney, L., Yang, J.Y., Zhang, J., 2004. Bioconductor: open software development for computational biology and bioinformatics. Genome Biol 5, R80.

Gould, J., Getz, G., Monti, S., Reich, M., Mesirov, J.P., 2006. Comparative gene marker selection suite. Bioinformatics 22, 1924–1925.

Irizarry, R.A., Hobbs, B., Collin, F., Beazer-Barclay, Y.D., Antonellis, K.J., Scherf, U., Speed, T.P., 2003. Exploration, normalization, and summaries of high density oligonucleotide array probe level data. Biostatistics 4, 249–264.

Kingsbury, J.S., Klimtchuk, E.S., Théberge, R., Costello, C.E., Connors, L.H., 2007. Expression, purification, and in vitro cysteine-10 modification of native sequence recombinant human transthyretin. Protein Expr. Purif. 53, 370–377.